The binding of imidazole in an azurin-like blue-copper site

Gastel, M. van; Coremans, J.W.A.; Mol, J.; Jeuken, L.J.C.; Canters, G.W.; Groenen, E.J.J.

JBIC (1999) 4:257–265

ORIGINAL ARTICLE

M. van Gastel · J. W. A. Coremans · J. Mol
L. J. C. Jeuken · G. W. Canters · E. J. J. Groenen

The binding of imidazole in an azurin-like blue-copper site

Received: 27 October 1998 / Accepted: 9 February 1999

Abstract Frozen solutions of the azurin mutant His117Gly in the presence of excess of methyl-substituted imidazoles have been investigated by electron spin-echo envelope modulation (ESEEM) spectroscopy at 9 GHz. The addition of imidazole is known to reconstitute a blue-copper site and variation of the non-protein bound ligand [*N*-methyl-, 2-methyl-, 4(5)-methylimidazole] has allowed the study of the copper-imidazole binding as a model for histidine binding in such sites. Quadrupole and hyperfine tensors of the remote nitrogen of the imidazoles have been determined. The quadrupole tensors indicate that the methyl-substituted imidazoles in the mutant adopt the same orientation relative to copper as the histidine-117 in the wild-type protein. Analysis of the hyperfine tensors in terms of spin densities reveals that the spin density on the remote nitrogen of the substituted imidazole has σ and a variable π character, depending on the position of the methyl group. For azurin the corresponding spin density is of virtually pure σ character. In conclusion, blue-copper sites show subtle variations as regards the histidine/imidazole centred part of the wavefunction of the unpaired electron.

Key words Electron spin-echo envelope modulation · Azurin · Blue-copper proteins

M. van Gastel · J. W. A. Coremans · J. Mol
E. J. J. Groenen (✉)
Centre for the Study of Excited States of Molecules
University of Leiden, Huygens Laboratory, P. O. Box 9504
2300 RA Leiden, The Netherlands
e-mail: mat@molphys.leidenuniv.nl
Fax: +31-71-5275819

G. W. Canters (✉) · L. J. C. Jeuken
Department of Chemistry, University of Leiden
Gorlaeus Laboratories, P. O. Box 9502, 2300 RA Leiden
The Netherlands
e-mail: canters@chem.leidenuniv.nl
Fax: +31-71-5274526

Introduction

Blue-copper proteins function in redox-reaction chains in bacteria. Their active centre contains a single copper ion whose oxidation state switches between I and II in the electron transfer process. The copper ion has a remarkable coordination that is responsible for the characteristic blue colour of this class of copper proteins. From X-ray studies on single crystals of several type I blue-copper proteins [1, 2, 3, 4], a high degree of structural similarity is found for the coordination of the metal. The copper ion is ligated equatorially by the nitrogens of two histidines and the sulfur of a cysteine, at distances of about 1.9 and 2.2 Å, respectively. The structure of the copper site of oxidised azurin from *Pseudomonas aeruginosa* obtained from X-ray diffraction [1] is shown in Fig. 1, where it is seen that the metal ion is bound to histidines-46 and -117 and cysteine-112, while the axial positions are taken by methionine-121 and glycine-45. The binding to glycine-45 is weak and unique for azurin and the site can best be described as a distorted bipyramid.

Some years ago, it was shown that the replacement of histidine-117 by a glycine using site-directed mutagenesis creates an aperture in the hydrophobic surface patch of azurin by which the copper centre becomes amenable to direct manipulation through the binding of external ligands [5]. Addition of, for example, imidazole to a solution of the H117G mutant fills up the aperture and leads to a copper site that gives a visible absorption spectrum and an X-band EPR spectrum that are characteristic of azurin [6]. In other words, to the extent as measured by these techniques, the external ligand seems to restore the copper coordination present in the wild-type protein. Here we report on an electron spin-echo envelope modulation (ESEEM) study of the azurin mutant H117G to further characterise the binding of the ligand at position 117 to copper(II) and the role of the protein therein.

Recently we have studied the electronic structure of the oxidised copper site of azurin in a series of electron

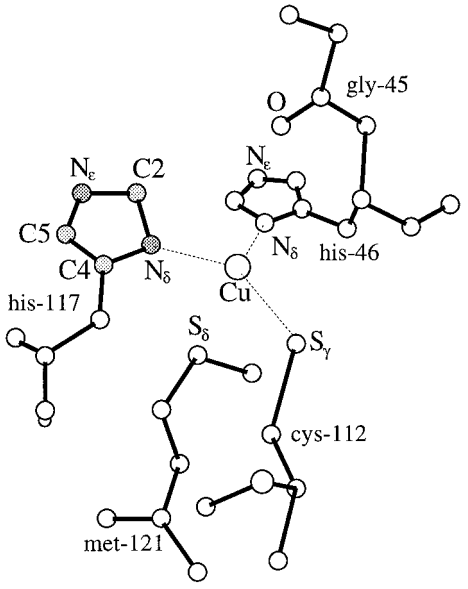

Fig. 1 The structure of the copper site of azurin from *Pseudomonas aeruginosa*. The imidazole of histidine-117 is *shaded*

spin-echo experiments. The *g*-tensor has been obtained from a single-crystal ESE-detected EPR study at 95 GHz [7]. The hyperfine and quadrupole tensors of the histidyl nitrogens coordinated to copper have been obtained from ESEEM at 95 GHz on a single crystal [8] and those of the remote histidyl nitrogens from a combination of pulsed ENDOR at 95 GHz [9, 10] on a single crystal and ESEEM at 9 GHz on a frozen solution [11]. The latter study revealed that three nitrogens contribute to the spin-echo modulations at 9 GHz. The largest contribution stems from the remote nitrogen of histidine-117. This observation makes the ESEEM technique particularly suited for the study of the externally added ligand in the reconstituted H117G mutant, because this ligand occupies the position related to that of histidine-117 in wild-type azurin. As reported previously [11], addition of imidazole to H117G leads to an ESEEM spectrum that is virtually identical to that of native oxidised azurin. Through variation of the external ligand added to the H117G solution and analyses of the corresponding one- and two-dimensional ESEEM spectra, we have obtained information about the histidine binding and electron delocalisation in blue-copper proteins.

Here we consider methylated imidazoles, i.e., *N*-methyl-, 2-methyl- and 4(5)-methylimidazole. The nomenclature H117G(Im) will be used to represent H117G with either 2-methylimidazole, *N*-methylimidazole or 4(5)-methylimidazole added externally. From the ESEEM spectra, quadrupole and hyperfine tensors of the remote nitrogen of the imidazole ligand have been derived. Analysis of the quadrupole interaction reveals that the externally added methylimidazoles, although not bound to the protein backbone, occupy the same position relative to copper in the H117G mutants as the histidine-117 in azurin. Analysis of the hyperfine interaction provides insight into the spin-density distribution around the remote nitrogen. Significant differences in this distribution are observed for the various H117G(Im) complexes. For azurin the imidazole centred part of the wavefunction of the unpaired electron has virtually pure σ character; for the H117G(Im) systems, π character shows up to an extent that varies with the position of the methyl group.

Materials and methods

The preparation of the H117G mutant of azurin has been reported elsewhere [5, 12]. Solutions of H117G(Im) were prepared by adding excess of one of the substituted imidazoles to H117G solutions that were buffered to pH 6. The protein concentration was typically 3 mM.

Three-pulse ESEEM and two-dimensional ESEEM experiments were performed at 6 K on a Bruker ESP380E X-band spectrometer. Microwave frequencies were 9.63 GHz for H117G(2-methylimidazole), 9.75 GHz for H117G(N-methylimidazole) and H117G(4(5)-methylimidazole). The $\pi/2$ pulses had a length of 16 ns. The time τ between the first and second microwave pulse was 144 ns, as short as possible, and a few experiments were performed at higher τ values. In total, 2048 data points were acquired for the time T between the second and third pulse with a time increment of 8 ns. The starting value of T was 56 ns. Both the in-phase and out-of-phase components of the stimulated echo were measured as well as the zero level of the echo. The further treatment of the modulation patterns was performed in the same way as reported previously [11]. The ESEEM spectra obtained in this way are all represented as magnitude spectra. No window functions were used.

In the two-dimensional ESEEM experiments a four-step phase-cycling routine was used. For the first microwave pulse a $+-+-$ phase cycle was used, for the second $++--$, for the third $++++$, and for the detection of the echo a $+--+$ cycle, where $+$ and $-$ differ 180° in phase. In total, 128×1024 data points were acquired in the τ and T dimension with time increments of 24 ns and 8 ns, respectively. In 2D ESEEM, cross-peaks are expected at $(\nu_Q \pm \nu_{DQ},\nu_Q)$ and $(\nu_{DQ} \pm \nu_Q,\nu_{DQ})$ [13], where the first coordinate corresponds to the τ related frequency and the second to the T related frequency, ν_Q represents one out of the three frequencies in the cancelled manifold and ν_{DQ} the $\Delta M_I=2$ transition. Because of the sum and difference frequencies in the first coordinate, the cross-peaks are well away from the diagonal and can be used to find a set of frequencies that belongs to one nitrogen. The background of the two-dimensional modulation pattern was removed by subtracting a quadratic fit to the slices measured at fixed τ. After that a Hamming window function was used. Zero filling was performed to obtain 512×2048 data points that were subsequently Fourier transformed to obtain magnitude contour plots.

Details of the procedure to simulate the ESEEM spectra for different values of the magnetic field and of the time τ can be found elsewhere [11]. The simulations yield quadrupole and hyperfine tensors of the nitrogens that contribute to the ESEEM spectra . These tensors are defined in the principal axes system of the *g*-tensor (*xyz*) and, knowing the orientation of the *g*-tensor in the copper site [7], can be translated into any other coordinate system in the copper site.

Results

ESEEM spectra

The ESEEM spectra of frozen solutions of H117G(Im) at three magnetic-field positions in the ESE-detected

EPR spectrum are shown in Fig. 2b–d. The magnetic field positions are chosen such that the canonical orientations are probed where low field is close to g_z, intermediate field close to g_y and high field close to g_x (cf. Fig. 2). Similar spectra for wild-type azurin have been published previously [11], and are reproduced in Fig. 2a for comparison. Figure 3 shows ESEEM spectra of the H117G(Im) solutions at intermediate magnetic field for several values of τ. Two-dimensional ESEEM spectra of the same solutions are represented in Fig. 4. Both the positions of the cross-peaks and the corresponding fundamental frequencies are summarised in Table 1.

All ESEEM spectra are characterised by narrow bands below 2 MHz and broader features around 4 MHz, typical for nitrogen [14]. In the ESEEM spectrum of azurin a band is present at 2.8 MHz that is less pronounced in the ESEEM spectra of H117G(Im). The modulation depth for the H117G(Im) samples is larger than for azurin, leading to more intensity in the ESEEM spectra. The ESEEM spectra of H117G(Im) will now be described one by one.

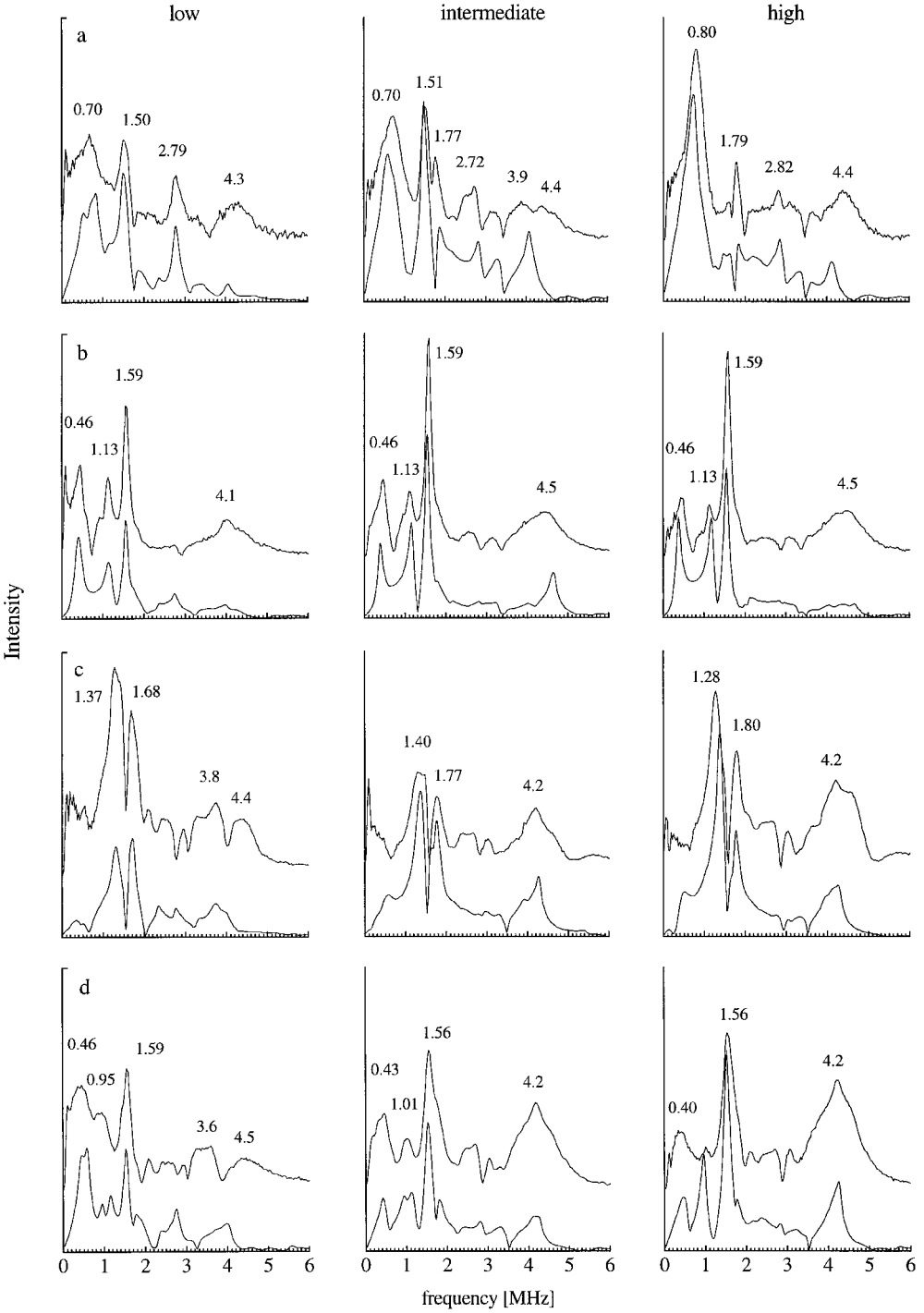

Fig. 2 Experimental and simulated ESEEM spectra of frozen solutions of **a** wild-type azurin, **b** H117G(2-methylimidazole), **c** H117G(N-methylimidazole) and **d** H117G(4(5)-methylimidazole). For the intensities to be comparable, the spectral intensity in **b** has to be multiplied by four, that in **c** and **d** by two. The *lower curve* in each panel represents the simulated spectrum. The microwave frequencies were 9.748 GHz for **a**, 9.631 GHz for **b**, 9.750 GHz for **c** and 9.748 GHz for **d**, while the τ time was 144 ns for all experiments. The corresponding *g*-values are (from low to high magnetic field) 2.23, 2.06 and 2.04 for **a** and 2.23, 2.06 and 2.03 for **b–d**. For the simulations, the hyperfine and quadrupole tensors of the remote nitrogen of the imidazole are given in Table 2, those of the remote nitrogen of histidine-46 and a backbone nitrogen in Table II of van Gastel et al. [11]. Other parameters used in the simulations concern *g*-strain ($W_x = 0.5$ mT, $W_y = 0.9$ mT and $W_z = 3.8$ mT), the hyperfine interaction on copper (175 MHz) and the bandwidth of the microwaves (0.3 mT)

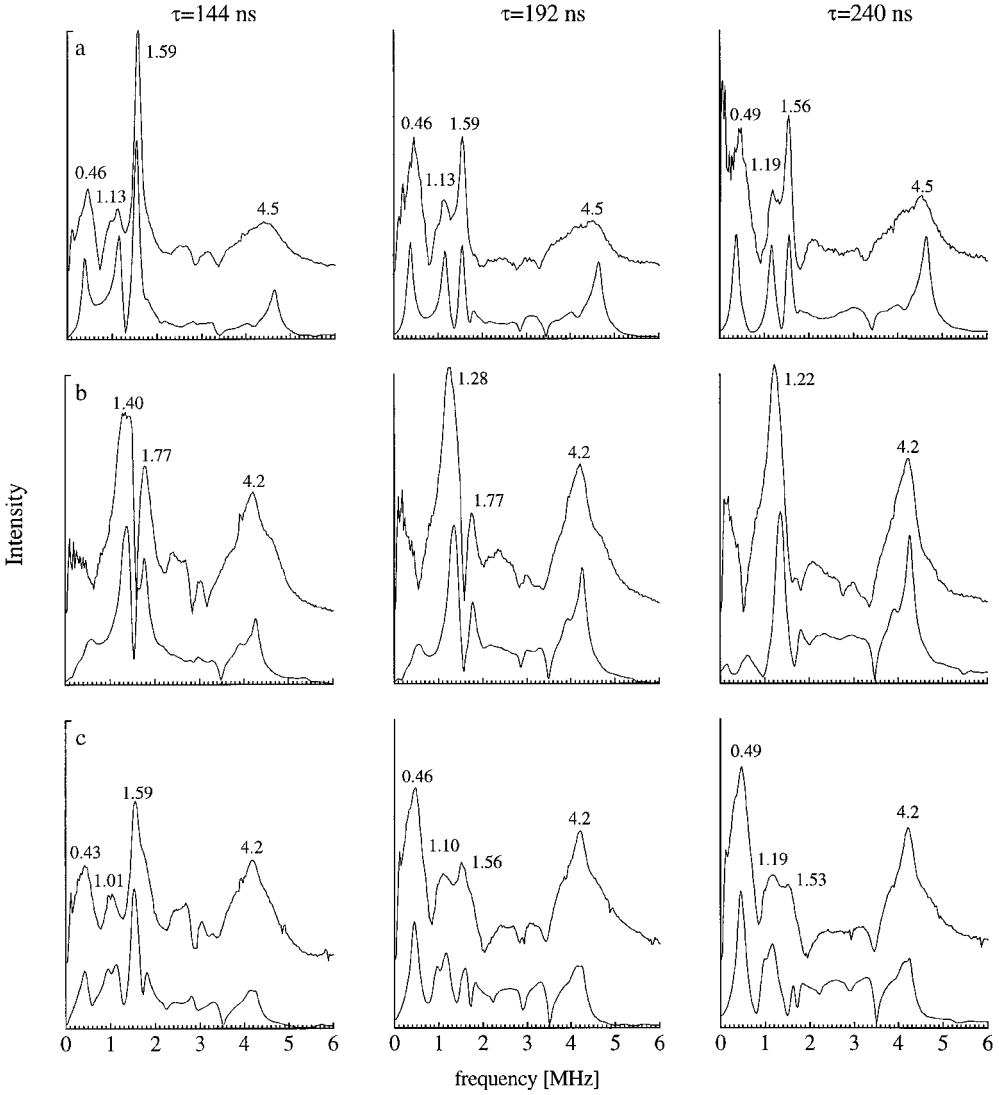

Fig. 3 Experimental and simulated ESEEM spectra for **a** H117G(2-methylimidazole, **b** H117G(*N*-methylimidazole) and **c** H117G(4(5)-methylimidazole) at intermediate magnetic field ($g=2.06$) for different τ values. The spectrum in the *third column* of **c** has been recorded for $\tau=208$ ns. The *upper traces* are the experimental spectra. The corresponding microwave frequencies are given in the caption of Fig. 2

For H117G(2-methylimidazole) the modulation depth is largest (Fig. 2b). Narrow bands are observed at 0.46, 1.13 and 1.59 MHz whose frequencies and intensities are essentially the same at different magnetic fields. At low magnetic field a broad feature is visible at 4.1 MHz that shows up at 4.5 MHz for intermediate and high field. For higher values of τ (Fig. 3a), different intensities are observed, somewhat lower for the band at 1.59 MHz and somewhat higher for the bands at 0.46 and 4.5 MHz. The 2D-ESEEM spectrum (Fig. 4a) reveals two cross-peaks (I and II) that correlate 1.59 MHz to 4.66 MHz.

For H117G(N-methylimidazole), the ESEEM spectrum at low magnetic field (Fig. 2c) shows two intense bands at 1.37 and 1.68 MHz and weaker, broader features between 3.2 and 4.4 MHz. At higher fields the intensity in the latter range shows up as a broad band with a maximum at 4.2 MHz. At the intermediate field and highest value of τ (Fig. 3b), the lowest-frequency band is found at 1.22 MHz while the second lowest band has disappeared. In the 2D-ESEEM spectrum (Fig. 4b), five cross-peaks have been recognised. The strongest, indicated by I and II, correlate 1.31 MHz to 4.3 MHz and 1.77 MHz to 4.3 MHz.

For H117G(4(5)-methylimidazole) the modulation depth is comparable to that for H117G(*N*-methylimidazole). The ESEEM spectrum at low magnetic field (Fig. 2d) shows intense bands at 0.46, 0.95 and 1.59 MHz and weaker, broader features between 3.2 and 4.7 MHz. Going to higher magnetic fields, the first two bands lose intensity, while the broad features form a more intense band with a maximum at 4.2 MHz, as for H117G(*N*-methylimidazole). As Fig. 3c shows, the intensity of the band at 0.43 MHz increases at higher values of τ while the intensity of the band at 1.59 MHz decreases and becomes comparable to that of the band at around 1.1 MHz. The 2D-ESEEM spectrum (Fig. 4c) shows strong correlation peaks relating frequencies 1.59 and 4.2 MHz (I) and 1.65 and 4.5 MHz (II).

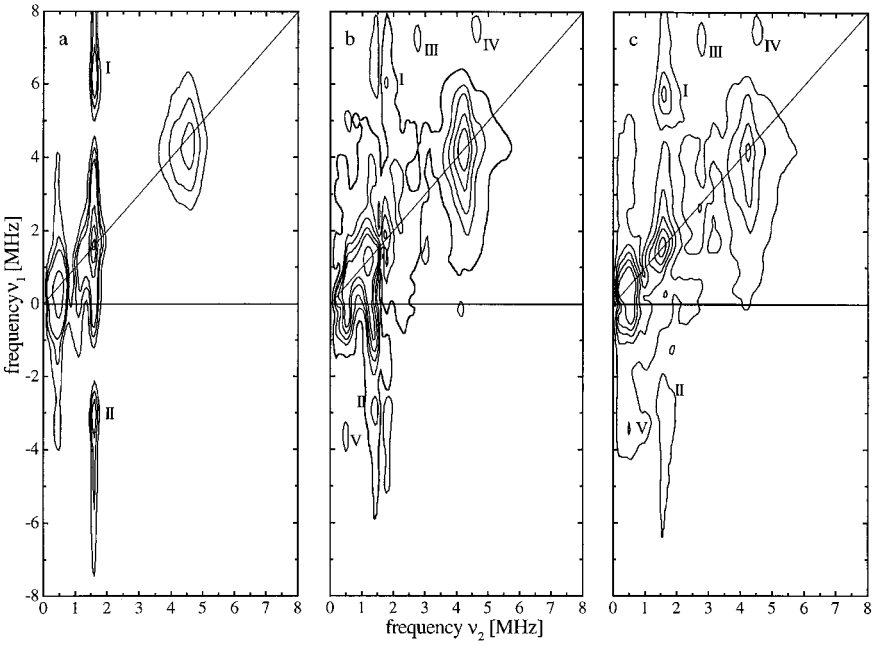

Fig. 4 Two dimensional ESEEM spectra of **a** H117G(2-methylimidazole), **b** H117G(*N*-methylimidazole) and **c** H117G(4(5)-methylimidazole) measured at intermediate magnetic field. The corresponding microwave frequencies are given in the caption of Fig. 2. The *roman numerals* label the cross-peaks (cf. Table 1)

Table 1 Cross-correlation peaks (ν_1, ν_2) in MHz for the 2D-ESEEM spectra of H117G(Im) and the corresponding fundamental frequencies. The first coordinate represents the τ related frequency

	H117G(2-methylimidazole)				H117G(*N*-methylimidazole)				H117G(4(5)-methylimidazole)			
	Cross-peak	Fundamental frequencies			Cross-peak	Fundamental frequencies			Cross-peak	Fundamental frequencies		
I	1.59, 6.25	1.59	4.66	I	1.77, 6.04	1.77	4.27	I	1.59, 5.76	1.59	4.17	
II	1.58,–3.09	1.58	4.67	II	1.39,–2.92	1.39	4.31	II	1.65,–2.81	1.65	4.46	
				III	2.74, 7.29	2.74	4.55	III	2.76, 7.30	2.76	4.54	
				IV	4.61, 7.58	2.97	4.61	IV	4.52, 7.55	3.03	4.52	
				V	0.50,–3.61	0.50	4.11	V	0.50,–3.44	0.50	3.94	

Simulations

Recently, the ESEEM spectrum of azurin has been interpreted and contributions of three nitrogens have been recognised [11]. The dominant contribution stems from the remote nitrogen of histidine-117 with bands at 0.7 and 1.5 MHz, while weaker contributions stem from the remote nitrogen of histidine-46 with a band at 1.8 MHz and a backbone nitrogen with a band at 2.8 MHz (cf. Fig. 2a). On the basis of this work, the complicated ESEEM spectra of H117G(Im) have been analysed through spectral simulations.

The simulations are performed in the principal axes system of the *g*-tensor (*xyz*). As a starting point, the following approach was used. Because of the apparent restoration of the blue-copper site after addition of one of the methylated imidazoles to H117G, the nitrogens are assumed to contribute in the same way to the ESEEM spectra of H117G(Im) as they do in the case of wild-type azurin except for the remote nitrogen of the external additive. Therefore, nuclear hyperfine and quadrupole parameters for the remote nitrogen of histidine-46 and the backbone nitrogen are taken from the ESEEM study on azurin. The initial values of the quadrupole parameters e^2qQ and η for the imidazole nitrogen are calculated from the cross-peaks observed in the 2D-ESEEM spectra. Both the hyperfine tensor and the quadrupole tensor of this nitrogen have been varied until a change in any parameter did not significantly improve the simulation. Slight optimisations of e^2qQ and η were found to be necessary in order to reproduce the ESEEM spectra.

The simulations are represented in Fig. 2b–d and 3a–c (lower traces) and the hyperfine and quadrupole parameters obtained for the remote nitrogen of the added imidazole are given in Table 2. Those for azurin (Fig. 3a and Table 2) have been reproduced from van Gastel et al. [11]. The simulations reproduce most features in the ESEEM spectra and the changes with field (Fig. 2) and with τ time (Fig. 3). Intrinsic shortcomings of the ESEEM simulations, especially with regard to the frequency region between 4 and 5 MHz, have been discussed previously [11]. For H117G(*N*-methylimidazole) the hyperfine tensor is almost axial and only the

Table 2 Principal values (MHz) of the hyperfine and quadrupole tensors and orientations of the principal axes of the hyperfine ($x''y''z''$) and quadrupole ($x'y'z'$) tensors of the remote nitrogens with respect to the principal axes system of the *g*-tensor (xyz). The 2-methyl in column 1 refers to the remote nitrogen of the imidazole in H117G(2-methylimidazole) and the other entries in column 1 have similar meaning. His-117 refers to the remote nitrogen of histidine-117 in azurin, and the data are reproduced from van Gastel et al. [11]. Note that the sign of the z component of the x'' axis for this nitrogen (–0.091) is in error in this reference. Error margins are typically ±0.1 MHz for the principal values of the hyperfine and quadrupole tensors and ±15° for the orientation of the principal axes of these tensors. The hyperfine tensor of H117G(*N*-methylimidazole) is almost axial and the orientation of the y'' and z'' axes could not be determined. The definition of $x'y'z'$ for the Nε of His-117 in azurin deviates from the convention $|Q_{x'x'}| < |Q_{y'y'}| < |Q_{z'z'}|$. This facilitates the comparison of the quadrupole tensor with those of the H117G(Im) complexes but leads to a value of η larger than one

	A_{iso}/h	$A_{x''x''}/h$	$A_{y''y''}/h$	$A_{z''z''}/h$		x	y	z
2-Methyl	2.00	2.36	2.17	1.46	x''	0.275	−0.949	0.156
					y''	0.689	0.308	0.657
					z''	−0.671	−0.073	0.738
N-Methyl	1.60	1.91	1.47	1.41	x''	−0.657	−0.753	0.040
					y''			
					z''			
4(5)-Methyl	1.60	1.91	1.57	1.31	x''	−0.844	−0.440	0.305
					y''	0.463	−0.313	0.829
					z''	−0.270	0.841	0.468
His-117	1.40	1.76	1.36	1.07	x''	−0.333	−0.939	−0.091
					y''	0.644	−0.156	−0.749
					z''	0.689	−0.308	0.657
	e^2qQ/h	η	$Q_{x'x'}$	$Q_{y'y'}$	$Q_{z'z'}$			
2-Methyl	−1.77	0.40	0.27	0.62	−0.89	x'	0.331	−0.899	−0.288
						y'	0.678	0.438	−0.590
						z'	0.656	0.000	0.755
N-Methyl	−2.00	0.15	0.43	0.58	−1.00	x'	−0.145	−0.867	−0.476
						y'	0.887	0.099	−0.452
						z'	0.439	−0.488	0.755
4(5)-Methyl	−1.65	0.60	0.17	0.66	−0.83	x'	−0.807	−0.458	0.372
						y'	0.213	−0.814	−0.541
						z'	0.550	−0.357	0.755
His-117	−1.38	1.10	−0.03	0.72	−0.69	x'	−0.240	−0.762	−0.601
						y'	0.797	0.199	−0.571
						z'	0.555	−0.616	0.559

orientation of the principal x'' axis is determined with sufficient accuracy. The definition of the principal axes of the tensors is such that the principal values conform to the convention $|A_{x''x''}| > |A_{y''y''}| > |A_{z''z''}|$ and $|Q_{x'x'}| < |Q_{y'y'}| < |Q_{z'z'}|$. Variation of any of the hyperfine or quadrupole parameters of the remote nitrogen of histidine-46 or of the backbone nitrogen did not significantly improve the simulations. The parameters for these nitrogens correspond to those in Table II of van Gastel et al. [11].

Discussion

In this section we first discuss the quadrupole and hyperfine interaction of the remote nitrogen of imidazole in the H117G(Im) systems and compare the results with those of histidine-117 in azurin. Subsequently, we focus on the implications for the description of the binding of imidazole/histidine in blue-copper centres.

The simulations in Figs. 2 and 3 of the ESEEM spectra of H117G(Im) have revealed that the dominant contribution to the modulations stems from the remote nitrogen of the substituted imidazole and the hyperfine and quadrupole tensors of this nitrogen have been obtained. The value of a_{iso} of this nitrogen in the three H117G(Im) complexes is consistently bigger than that of the remote nitrogen of histidine-117 in azurin (cf. Table 2). Consequently, the hyperfine interaction comes closer to cancellation of the Zeeman interaction [15], which explains the larger modulation depth compared to azurin and the fact that the contributions of the remote nitrogen of histidine-46 and the backbone nitrogen to the ESEEM spectra, already relatively small for azurin, become minor for the present systems.

The values of the quadrupole parameters e^2qQ and η of the imidazole nitrogen in H117G(Im) resemble those of the corresponding nitrogens of substituted imidazoles in copper(II)-diethylenetriamine [16]. Surprisingly, the quadrupole parameters e^2qQ and η of azurin and H117G(imidazole) are alike [11] while those of azurin and H117G(4(5)-methylimidazole) are not, although for azurin the imidazole ring of histidine-117 is bound to the protein at the 4-position. Apparently, the electron-withdrawing effect of the backbone neutralises the effect of the side-chain CH_2 group on the electron distribution within the imidazole part of the histidine.

Owing to symmetry, the quadrupole interaction of the remote nitrogen, determined by the nuclear quadrupole moment and the local electron distribution, has one of its principal axes perpendicular to the imidazole plane. Model calculations on the substituted imidazoles [17] show that this axis corresponds to the largest principal value (z'). Consequently, the direction of the z' axis has been used to determine the orientation of the imidazoles with respect to xyz for the H117G(Im) systems. The orientation of the z' axes in the principal axes system xyz of the g-tensor for the imidazole nitrogen in H117G(*N*-methylimidazole) and H117G(4(5)-methylimidazole) is similar to that for the remote nitrogen of histidine-117 in azurin (cf. Table 2), but the orientation of the z' axis of the corresponding nitrogen in H117G(2-methylimidazole) deviates significantly. The latter observation implies that either the 2-methylimidazole has another orientation in the mutant than the imidazole of histidine-117 in azurin or the orientation of the reference axes xyz of the g-tensor with respect to the copper site is different for azurin and H117G(2-methylimidazole). The latter explanation is most probable for three reasons. Firstly, no rotation around the copper-Nδ axis (cf. Fig. 1) is sufficient to position the z' axis perpendicular to the imidazole plane. Secondly, if we rotate the x and y axes for H117G(2-methylimidazole) by 48° around z compared to their orientation for azurin, the orientation of the z' axis for H117G(2-methylimidazole) *with respect to the copper site* becomes similar to that of the z' axis for azurin. H117G(Im) and azurin have almost axial EPR spectra. For azurin the small rhombicity has been resolved at W-band frequency (95 GHz) and the orientation of the g-tensor principal axes with respect to the copper site has been obtained with an accuracy of 3° [7]. The z axis, corresponding to the highest g-value, is almost perpendicular to the equatorial plane of the copper site, spanned by the two copper-coordinated nitrogens and the sulfur of the cysteine. The orientation of the x and y axes is very sensitive to small changes in the electronic wavefunction owing to the near degeneracy of g_x and g_y. Thirdly, the angle between the z axis and the z' axis is the same for all H117G(Im) complexes (direction cosine equals 0.755, cf. Table 2), which points to a comparable orientation of the imidazole in the three complexes. Most likely, the imidazoles in the H117G(Im) complexes are in the same position relative to copper as the histidyl imidazole in azurin while the x and y axes for H117G(2-methylimidazole) are rotated with respect to those for azurin. In the simulations of the ESEEM spectra of the H117G(2-methylimidazole) complex the hyperfine and quadrupole parameters for the remote nitrogen of histidine-46 and the backbone nitrogen are taken the same as for azurin, because the remote nitrogen of 2-methylimidazole largely dominates the ESEEM spectra.

The hyperfine tensor of the remote nitrogen of the imidazole in the H117G(Im) systems depends on the position of the methyl group in the imidazole (cf. Table 2). For the methyl group in the 2-position, both the isotropic part and the anisotropy of the hyperfine interaction are largest. In order to derive information about the electron-spin distribution from the hyperfine tensors, we have used a simple model to describe their anisotropy. For comparison a similar analysis has been performed for azurin. In the model the anisotropic part of the tensor is written as a sum of the contributions of spin densities ρ_i in atomic orbitals $|\phi_i\rangle$:

$$\frac{\vec{\vec{A}}_{\text{aniso}}}{h} = g(^{14}\text{N})\,\beta_n\, g_e\,\beta_e \sum_i \rho_i \left\langle \phi_i \left| \frac{3\hat{r}\hat{r} - \vec{\vec{E}}}{r^3} \right| \phi_i \right\rangle \qquad (1)$$

where $\vec{r}$ is the position of the electron spin with respect to the nucleus ($\hat{r} \equiv \vec{r}/r$), $\vec{\vec{E}}$ is the unit matrix, β_n and β_e are the nuclear and Bohr magneton, and $g(^{14}\text{N})$ and g_e are the nuclear and electronic g-values. For the on-centre contribution to the anisotropic tensor, i.e., the interaction between the nuclear spin of the remote nitrogen and the electron-spin density in the orbitals on that atom, the electron-spin density has been modelled by three in-plane σ orbitals and one out-of-plane p orbital and the integral of Eq. 1 has been evaluated explicitly [18]. The methyl group affects the spin-density distribution in the imidazole in a way dependent on its position. Because explicit incorporation of the spin densities on the carbon atoms of the imidazole into the model would lead to too many parameters, we have taken the effect of alkylation into account by allowing different spin densities in the three σ orbitals on the nitrogen. Besides the contribution of the spin density on the remote nitrogen to the hyperfine tensor, contributions of the spin densities on the copper and the copper-coordinated nitrogen of the imidazole (histidine-117 in the case of azurin) have been considered. To calculate these two-centre terms, the spin densities have been replaced by point spins. The spin density on the copper and the copper-coordinated nitrogen have been taken from a previous study [10] and kept fixed at 60% and 9.4%, respectively. Although the amount of spin density on the sulfur of cysteine-112 is significant, it makes an insignificant contribution to the anisotropic tensor [10].

The model allows a quantitative evaluation of the anisotropic hyperfine tensors in terms of the three σ spin densities and one π spin density on the remote nitrogen if we apply the constraint that the s spin density (taken equal to one third of the total σ spin density) reproduces the experimental isotropic hyperfine interaction (taken to be 1062 MHz for unit spin density in a 2s orbital on nitrogen [19]). The results of the analyses for the various H117G(Im) complexes and azurin are represented in Table 3. The tensor elements are given in a local axes system abc where a points in the N-H direction (N-CH_3 for *N*-methylimidazole), c is perpendicular to the plane of imidazole and b perpendicular to a and c and in the direction of the C2 carbon (cf. Fig. 1). For H117G(2-methylimidazole), the anisotropic tensor has been translated into the abc axes system un-

Table 3 Anisotropic hyperfine tensors (MHz) of the remote nitrogen (N) of the imidazole for the H117G(Im) complexes and the histidine-117 nitrogen for azurin in a local axes system *abc*, in which *a* is the N-H direction, *c* is perpendicular to the imidazole plane and *b* is the in-plane axis pointing to the direction of C-2. (a) The calculated contribution of spin density on the N to the anisotropic hyperfine tensor, the calculated and experimental total anisotropic hyperfine tensors. In the first column are given the calculated π and total σ spin densities on the N for which the error margin is 0.001. (b) Contributions of the spin densities on copper and the copper-coordinated nitrogen to the anisotropic hyperfine tensor of the N which have been assumed equal for all systems (spin densities are taken from Coremans et al. [10])

(a)		Nε			Calculated tensor			Experimental tensor		
		a	*b*	*c*	*a*	*b*	*c*	*a*	*b*	*c*
2-Methyl										
$\rho(\pi)=0.0049$	*a*	−0.217	−0.317	0.000	−0.063	−0.436	0.004	−0.063	−0.436	0.098
$\rho(\sigma)=0.0056$	*b*	−0.317	−0.058	0.000	−0.436	−0.107	−0.002	−0.436	−0.107	0.048
	c	0.000	0.000	0.275	0.004	−0.002	0.170	0.098	0.048	0.170
N-Methyl										
$\rho(\pi)=0.0013$	*a*	−0.092	−0.128	0.000	0.061	−0.247	0.004	0.061	−0.247	0.012
$\rho(\sigma)=0.0045$	*b*	−0.128	0.111	0.000	−0.247	0.063	−0.002	−0.247	0.063	0.003
	c	0.000	0.000	−0.019	0.004	−0.002	−0.125	0.012	0.003	−0.125
4(5)-Methyl										
$\rho(\pi)=0.0023$	*a*	−0.375	−0.063	0.000	−0.221	−0.182	0.004	−0.221	−0.182	−0.027
$\rho(\sigma)=0.0045$	*b*	−0.063	0.295	0.000	−0.182	0.247	−0.002	−0.182	0.247	−0.010
	c	0.000	0.000	0.079	0.004	−0.002	−0.026	−0.027	−0.010	−0.026
His-117										
$\rho(\pi)=-0.0005$	*a*	0.135	−0.019	0.000	0.289	−0.137	0.004	0.289	−0.137	0.067
$\rho(\sigma)=0.0039$	*b*	−0.019	0.056	0.000	−0.137	0.008	−0.002	−0.137	0.008	−0.091
	c	0.000	0.000	−0.191	0.004	−0.002	−0.297	0.067	−0.091	−0.297

(b)		Cu ($\rho=0.6$)			Nδ ($\rho=0.094$)		
		a	*b*	*c*	*a*	*b*	*c*
	a	0.063	−0.065	0.004	0.090	−0.054	0.001
	b	−0.065	−0.013	−0.002	−0.054	−0.035	0.000
	c	0.004	−0.002	−0.050	0.001	0.000	−0.055

der the assumption, based on the analysis of the quadrupole tensor, that *x* and *y* are rotated by 48° with respect to *x* and *y* for azurin. The model calculations reproduce the experimental tensors except for the small *ac* and *bc* elements. The calculated contribution of the spin density on the remote nitrogen to these elements is necessarily zero as a result of the way we have modelled the spin density on this atom. In Table 3 the total σ spin density $\rho(\sigma)$ and the π spin density $\rho(\pi)$ on the remote nitrogen (Nε) and the summed contribution of these spin densities to the calculated anisotropic hyperfine tensor are specified for each complex. For completeness also the contribution of the spin densities on copper and the coordinated nitrogen (Nδ) are given and it is seen that the contribution of the spin density on the remote nitrogen largely determines the anisotropic hyperfine tensors. The total spin density on the latter atom is larger for the three H117G(Im) systems than for azurin. The model provides an interpretation of the variation of the hyperfine tensor of the remote nitrogen with the position of the methyl group in the imidazole, though in view of the simplifications in the model the quantitative results should be considered with caution. The most striking observation concerns the σ/π character of the spin density. The ratio $\rho(\pi)/\rho(\sigma)$ is found to depend on the position of the methyl group, ranging from 0.79 for H117G(2-methylimidazole) to 0.29 for H117G(*N*-methylimidazole), while the amount of π spin density is virtually zero for azurin. The observation that the σ/π character of the spin density for H117G(2-methylimidazole) deviates the most from that for azurin is in line with the earlier suggestion, based on the quadrupole interaction, of a significant rotation of the principal *x* and *y* axes of the *g*-tensor for H117G(2-methylimidazole) compared to those for azurin.

The variation of the π-character of the spin density on the remote nitrogen is intriguing in view of the description of the binding of the imidazole/histidine to copper. Quantum-chemical calculations have indicated that the ground-state wavefunction of the unpaired electron in the oxidised blue-copper site concerns an orbital mainly localised on the copper and the sulfur of cysteine [20, 21, 22]. In these calculations the bonding of the sulfur to copper in this orbital is of π character, while that of nitrogen to copper is of σ character. For azurin our observation supports the σ character of the histidine part of the half-filled molecular orbital. When we consider the variation of $\rho(\pi)$ and $\rho(\sigma)$ in Table 3, it becomes clear that the binding of imidazole to copper is subtle and becomes modified even by the introduction of a methyl group in the imidazole. The substitution of a methyl group changes the energy of the molecular orbitals of imidazole, and thereby the participation

of the σ and π molecular orbitals in the wavefunction of the unpaired electron. This effect does not alter the EPR spectrum, nor the visible absorption spectrum, but shows up in the ESEEM spectrum which monitors particularly the part of the wavefunction located on the imidazole.

Conclusion

The investigation by one- and two-dimensional ESEEM spectroscopy of the His117Gly mutant of azurin after addition of various methyl-substituted imidazoles has provided deeper insight into the binding of histidines/imidazoles in oxidised blue-copper sites. At X-band frequencies the ESEEM technique is especially sensitive to the remote nitrogens of the copper-ligated imidazoles and probes the part of the wavefunction of the unpaired electron that is delocalised over this ligand. From the quadrupole tensors that have been obtained from simulations of the ESEEM spectra of the various H117G(Im) complexes, we have found that the externally added imidazole, although not bound to the protein, occupies the same position relative to copper as histidine-117 for azurin. For H117G(2-methylimidazole) the x and y principal axes of the g-tensor are rotated by 48° around z compared to those for azurin. From the analysis of the hyperfine tensors it has become apparent that subtle differences exist regarding the type of binding of imidazole to copper in the H117G(Im) systems and azurin. The amount of π spin density compared to σ spin density on the remote nitrogen of the imidazole varies strongly. For the H117G(2-methylimidazole) complex the amount of π spin density is almost as big as the amount of σ spin density, while for wild-type azurin the corresponding electron-spin density on imidazole has almost solely σ character. The observation of σ spin-density is of relevance for the interpretation of the hyperfine-shifted signals in the proton NMR spectra of paramagnetic blue-copper proteins [23].

Understanding the electron transport function of blue-copper proteins on a molecular level requires a detailed knowledge of the electronic wavefunction of the unpaired electron. The metal sites to be considered are big for present-day ab initio quantum chemistry. Such calculations on a truncated copper site are in progress in our laboratory and the knowledge of observables like the g-tensor and the hyperfine tensors allows a critical judgement of the quality of the wavefunctions. The subtle changes observed for the H117G(Im) complexes upon variation of the external ligand have been found most useful in this respect [24].

Note added in proof Recent 9 GHz Hyperfine Sublevel CORrelation spEctroscopy (HYSCORE) and Electron Nuclear DOuble Resonance (ENDOR) experiments for azurin show that the intensity around 4.5 MHz in the ESEEM spectra of azurin and H117G(Im) does not only stem from the $\Delta M_I = 2$ transition of the weakly coupled nitrogens, but also from the transitions of the β protons of cysteine-112 for which the hyperfine couplings are about 20 MHz in magnitude.

Acknowledgements The authors are indebted to B. Buijssefor his contribution to the simulations in the initial stage of the project. This work has been performed under the auspices of the BIOMAC Research school of the Leiden and Delft Universities and was supported by the Netherlands Foundation for Chemical Research (SON) with financial aid from the Netherlands Organisation for Scientific Research (NWO).

References

1. Nar H, Messerschmidt A, Huber R, van de Kamp M, Canters GW (1991) J Mol Biol 221:765–772
2. Guss JM, Freeman HC (1983) J Mol Biol 169:521–563
3. Petratos K, Dauter Z, Wilson KS (1988) Acta Crystallogr B44:628–636
4. Hart PJ, Nersissian AM, Herrmann AG, Nalbandyan RM, Valentine JS, Eisenberg D (1996) Protein Sci 5:2175–2183
5. den Blaauwen T, van de Kamp M, Canters GW (1991) J Am Chem Soc 113:550–552
6. den Blaauwen T, Canters GW (1993) J Am Chem Soc 115:1121–1129
7. Coremans JWA, Poluektov OG, Groenen EJJ, Canters GW, Nar H, Messerschmidt A (1994) J Am Chem Soc 116:3097–3101
8. Coremans JWA, Poluektov OG, Groenen EJJ, Canters GW, Nar H, Messerschmidt A (1997) J Am Chem Soc 119:4726–4731
9. Coremans JWA, van Gastel M, Poluektov OG, Groenen EJJ, den Blaauwen T, van Pouderoyen G, Canters GW, Nar H, Hammann C, Messerschmidt A (1995) Chem Phys Lett 235:202–210
10. Coremans JWA, Poluektov OG, Groenen EJJ, Canters GW, Nar H, Messerschmidt A (1996) J Am Chem Soc 118:12141–12153
11. van Gastel M, Coremans JWA, Jeuken LJC, Canters GW, Groenen EJJ (1998) J Phys Chem A 102:4462–4470
12. van de Kamp M, Hali FC, Rosato N, Finazzi Agro A, Canters GW (1990) Biochim Biophys Acta 1019:283–292
13. Shane JJ, Höfer P, Reijerse EJ, de Boer E (1992) J Magn Reson 99:596–604
14. Mims WB, Peisach J (1978) J Chem Phys 69:4921–4930
15. Flanagan HL, Singel DJ (1987) J Chem Phys 87:5606–5616
16. Jiang F, McCracken J, Peisach J (1990) J Am Chem Soc 112:9035–9044
17. Garcia MLS, Smith JAS, Bavin PMG, Ganellin CR (1983) J Chem Soc Perkin Trans 2 1391–1399
18. Groenen EJJ, Buma WJ, Schmidt J (1989) Isr J Chem 29:99–108
19. Pople JA, Beveridge DI (1970) Approximate molecular orbital theory.
McGraw Hill, New York, pp 128–135
20. Shadle SE, Penner-Hahn JE, Schugar HJ, Hedman B, Hodgson KO, Solomon EI (1993) J Am Chem Soc 115:767–776
21. Pierloot K, de Kerpel JOA, Ryde U, Roos BO (1997) J Am Chem Soc 119:218–226
22. Larsson S, Broo A, Sjölin L (1995) J Phys Chem 99:4860–4865
23. Kalverda AP, Salgado J, Dennison C, Canters GW (1996) Biochemistry 35:3085–3092
24. van Gastel M, Coremans JWA, Sommerdijk H, van Hemert MC, Canters GW, Groenen EJJ (1999) to be published